

Low-Dimensional Analysis of a Kuramoto Model with Inertia and Hebbian Learning

Tachin Ruangkriengsin

*Department of Mathematics, University of California Los Angeles,
Los Angeles, California 90095, USA*

Mason A. Porter

*Department of Mathematics, University of California Los Angeles,
Los Angeles, California 90095, USA and
Santa Fe Institute, Santa Fe, New Mexico, 87501, USA*

arXiv:2203.12090v1 [math.DS] 22 Mar 2022

Abstract

We study low-dimensional dynamics of a Kuramoto model with inertia with Hebbian learning. In this model, the coupling strength between oscillators depends on the phase differences between oscillators and changes according to a Hebbian learning rule. We analyze the special case of two coupled oscillators, which yields a three-dimensional dynamical system, and classify the stability of its equilibrium points using linear stability analysis. We show that the system is dissipative and that all of its trajectories are eventually confined to a bounded region. We approximate the limiting behavior and demarcate the parameter regions of three qualitatively different behaviors of the system. Using insights from our analysis of the low-dimensional dynamics, we study the original high-dimensional system when we draw the intrinsic frequencies of the oscillators from Gaussian distributions with different variances.

Synchronization occurs ubiquitously in many systems [1], such as in electrical impulses of neurons and the flashing of fireflies. In response to changes in external environmental conditions, many systems of coupled oscillators adapt to enhance collective behavior. One example of adaptation is plasticity in networks of neurons, in which the synaptic strengths between neurons change based on their relative spike times or other features [2]. Another example of adaptation occurs in groups of fireflies [3], which have been modeled using coupled phase oscillators with inertia, which can reduce local synchronization speed while simultaneously facilitating global synchronization. We consider both plasticity and inertia by examining a modified version of the ubiquitous Kuramoto model of coupled oscillators [4]. To examine the interplay between oscillator plasticity and inertia, we mathematically analyze a small system of these coupled oscillators. We then use the results of this analysis to gain some insights into larger systems of these oscillators.

I Introduction

The analysis of systems of coupled oscillators has been used extensively to study collective behavior in many systems [1], such as flashing in groups of fireflies [5], synchronization of pedestrians on the Millennium Bridge [6, 7], pacemaker conduction [8], and singing in frogs

[9]. In 1975, Yoshiki Kuramoto proposed a model of coupled biological oscillators as a system of a first-order differential equations in which each variable corresponds to the phase of an oscillator [10]. In this model, which is now known as the Kuramoto model, he assumed that the natural frequency of each oscillator is chosen from a fixed probability distribution. He also assumed all-to-all coupling in these oscillators and each oscillator is influenced by each other oscillator by a force that depends sinusoidally on their phase difference.

One natural extension to the original Kuramoto model is to incorporate a second-order term to model inertia [11]. This extension was proposed as part of an adaptive model to explain the ability of the firefly *Pteroptyx malaccae* to synchronize its flashing with almost no phase difference [3]. Kuramoto models with inertia have also been used to study disordered arrays of Josephson junctions [12], decentralized power grids [13], and other phenomena. Following the setup in Tanaka et al. [14], we consider a Kuramoto model with inertia of the form

$$m_i \frac{d^2 \phi_i}{dt^2} + \frac{d\phi_i}{dt} = \omega_i + \frac{1}{N} \sum_{j=1, j \neq i}^N K_{ij} \sin(\phi_j - \phi_i), \quad i \in \{1, 2, \dots, N\}, \quad (1)$$

where $\phi_i \in [0, 2\pi)$ is the phase of the i th oscillator, ω_i is its intrinsic frequency, m_i is its mass, $K_{ij} = K_{ji}$ is the symmetric coupling strength between the i th and j th oscillator, and N is the number of oscillators.

In the original formulation of the Kuramoto model, the coupling strength K_{ij} is constant. However, this assumption is too restrictive for some problems. For example, in neuroscience, neurons exhibit synaptic plasticity when their strengths change in response to activity-dependent mechanisms [2]. According to Hebbian theory [15], the synaptic strength between two neurons increases when they are active simultaneously. Analogously, viewing regularly spiking neurons as oscillators, the coupling strength K_{ij} is enhanced if the relative phase difference between two coupled oscillators is small. Several studies [16–20] have proposed a variety of functions to model the dynamics of the coupling between oscillators based on Hebbian theory. We follow [16] and suppose that the coupling strengths satisfy

$$\frac{dK_{ij}}{dt} = \beta(\alpha \cos(\phi_j - \phi_i) - K_{ij}), \quad (2)$$

where $\alpha > 0$ is the *learning enhancement factor* and $\beta > 0$ is the *learning rate*.

Equations (1, 2) constitute a dynamical system with $N + \frac{(N-1)(N)}{2} = \frac{N(N+1)}{2}$ equations. We first consider the case $N = 2$ and study the resulting low-dimensional system. We then use these insights to briefly consider higher-dimensional situations.

Our paper proceeds as follows. In Section II, we perform linear stability analysis of equations (1, 2) when there are $N = 2$ oscillators. We verify its dissipation and contraction properties in Section III. In Section IV, we demarcate the different behaviors of this system in a two-dimensional parameter space. We briefly examine the coupled oscillator system for larger N in Section V. We conclude in Section VI.

II Linear Stability Analysis of a System of $N = 2$ Coupled Oscillators

We examine (1, 2) with $N = 2$ oscillators with identical masses. This yields the three-dimensional (3D) dynamical system

$$m \frac{d^2 \phi_1}{dt^2} + \frac{d\phi_1}{dt} = \omega_1 + \frac{1}{2} k \sin(\phi_2 - \phi_1), \quad (3)$$

$$m \frac{d^2 \phi_2}{dt^2} + \frac{d\phi_2}{dt} = \omega_2 + \frac{1}{2} k \sin(\phi_1 - \phi_2), \quad (4)$$

$$\frac{dk}{dt} = \beta(\alpha \cos(\phi_2 - \phi_1) - k), \quad (5)$$

where $k := K_{12} = K_{21}$. By taking the difference (3)–(4), we obtain differential equations for the phase difference $\phi := \phi_1 - \phi_2 \in [-\pi, \pi)$, the derivative $\gamma := \frac{d\phi}{dt} \in \mathbb{R}$ of the phase difference, and intrinsic-frequency difference $\omega := \omega_1 - \omega_2 \in \mathbb{R}$. By symmetry, we assume without loss of generality that $\omega \geq 0$.

We reduce the number of parameters in (3)–(5) by rescaling time and defining $\tilde{k} := k/\beta$, $\tilde{\alpha} = \alpha/\beta$, $\tilde{\omega} := \omega/\beta$, $\tilde{\gamma} := \gamma/\beta$, $\tilde{m} := \beta m$, and $\tilde{t} := \beta t$. These transformations absorb the parameter β , so we take $\beta = 1$ without loss of generality and obtain

$$\frac{d\phi}{dt} = \gamma, \quad (6)$$

$$\frac{d\gamma}{dt} = \frac{1}{m}(-\gamma + \omega - k \sin(\phi)), \quad (7)$$

$$\frac{dk}{dt} = \alpha \cos(\phi) - k, \quad (8)$$

where we drop the tildes from our notation for convenience.

We obtain the equilibrium points (ϕ^*, γ^*, k^*) of the dynamical system (6)–(8) by setting $\frac{d\phi}{dt} = \frac{d\gamma}{dt} = \frac{dk}{dt} = 0$. This yields $\gamma^* = -\gamma^* + \omega - k^* \sin(\phi^*) = 0$ and $\alpha \cos(\phi^*) - k^* = 0$. Simplifying yields

$$\sin(2\phi^*) = \frac{2\omega}{\alpha}. \quad (9)$$

This implies that the equilibrium points exist if and only if $\alpha \geq 2\omega$.

Because $\phi \in [-\pi, \pi)$, we obtain four equilibria: $P_1 = (\frac{1}{2} \arcsin(\frac{2\omega}{\alpha}), 0, \alpha \cos(\frac{1}{2} \arcsin(\frac{2\omega}{\alpha})))$, $P_2 = (\frac{\pi}{2} - \frac{1}{2} \arcsin(\frac{2\omega}{\alpha}), 0, \alpha \sin(\frac{1}{2} \arcsin(\frac{2\omega}{\alpha})))$, $P_3 = (-\pi + \frac{1}{2} \arcsin(\frac{2\omega}{\alpha}), 0, -\alpha \cos(\frac{1}{2} \arcsin(\frac{2\omega}{\alpha})))$, and $P_4 = (-\frac{\pi}{2} - \frac{1}{2} \arcsin(\frac{2\omega}{\alpha}), 0, -\alpha \sin(\frac{1}{2} \arcsin(\frac{2\omega}{\alpha})))$.

The Jacobian matrix for the linearization of (6)–(7) at the equilibrium points is

$$J(\phi^*, \gamma^*, k^*) = \begin{bmatrix} 0 & 1 & 0 \\ -\frac{k^*}{m} \cos(\phi^*) & -\frac{1}{m} & -\frac{\sin(\phi^*)}{m} \\ -\alpha \sin(\phi^*) & 0 & -1 \end{bmatrix} = \begin{bmatrix} 0 & 1 & 0 \\ -\frac{\alpha \cos^2(\phi^*)}{m} & -\frac{1}{m} & -\frac{\sin(\phi^*)}{m} \\ -\alpha \sin(\phi^*) & 0 & -1 \end{bmatrix}. \quad (10)$$

The eigenvalues λ of the Jacobian matrix satisfy

$$-\lambda(\lambda + 1)(\lambda + \frac{1}{m}) - \frac{\alpha \cos^2(\phi^*)}{m}(\lambda + 1) + \frac{\alpha \sin^2(\phi^*)}{m} = 0. \quad (11)$$

Using (9), we simplify equation (11) for each equilibrium point. The equilibrium points P_1 and P_3 both give

$$-2\lambda(\lambda + 1)(m\lambda + 1) - (\alpha + \sqrt{\alpha^2 - 4\omega^2})(\lambda + 1) + (\alpha - \sqrt{\alpha^2 - 4\omega^2}) = 0. \quad (12)$$

The equilibrium points P_2 and P_4 both give

$$-2\lambda(\lambda + 1)(m\lambda + 1) - (\alpha - \sqrt{\alpha^2 - 4\omega^2})(\lambda + 1) + (\alpha + \sqrt{\alpha^2 - 4\omega^2}) = 0. \quad (13)$$

When $\alpha = 2\omega$, we obtain $P_1 = P_2$ and $P_3 = P_4$. These mergers of equilibrium points yield saddle–node bifurcations that arise from the same characteristic equation:

$$\lambda(\lambda + 1)(m\lambda + 1) + \frac{\alpha\lambda}{2} = \lambda \left(m\lambda^2 + (m + 1)\lambda + 1 + \frac{\alpha}{2} \right) = 0, \quad (14)$$

which gives $\lambda = 0$ and $\lambda = \frac{-(m+1) \pm \sqrt{(m-1)^2 - 2m\alpha}}{2m}$.

When $\alpha > 2\omega$, we have the following proposition.

Proposition 1. *Consider the dynamical system (6)–(8) with $\alpha > 2\omega$. Let $u := \alpha + \sqrt{\alpha^2 - 4\omega^2}$ and $v := \alpha - \sqrt{\alpha^2 - 4\omega^2}$. The following statements hold:*

1. Let Γ_1 be the region in the (u, v) plane with $0 \leq v \leq u \leq \frac{2(m^2 - m + 1)}{3m}$ that is bounded by the curves

$$v = u - \frac{(m + 1 + \sqrt{4(m + 1)^2 - 6m(u + 2)})(\sqrt{4(m + 1)^2 - 6m(u + 2)} - 2(m + 1))^2}{54m^2},$$

$$v = u - \frac{(m + 1 - \sqrt{4(m + 1)^2 - 6m(u + 2)})(\sqrt{4(m + 1)^2 - 6m(u + 2)} + 2(m + 1))^2}{54m^2}.$$

If $(u, v) \notin \Gamma_1$, then the Jacobian matrix at the equilibria P_1 and P_3 has a negative real eigenvalue and two complex-conjugate eigenvalues with negative real part. Otherwise, the Jacobian matrix at the equilibria P_1 and P_3 has three negative real eigenvalues.

2. Let Γ_2 be the region in the (u, v) plane with $0 \leq v \leq u$ and $v \leq \frac{2(m^2-m+1)}{3m}$ that is bounded by the curves

$$u = v - \frac{(m+1 + \sqrt{4(m+1)^2 - 6m(v+2)})(\sqrt{4(m+1)^2 - 6m(v+2)} - 2(m+1))^2}{54m^2},$$

$$u = v - \frac{(m+1 - \sqrt{4(m+1)^2 - 6m(v+2)})(\sqrt{4(m+1)^2 - 6m(v+2)} + 2(m+1))^2}{54m^2}.$$

If $(u, v) \notin \Gamma_2$, the Jacobian matrix at the equilibria P_2 and P_4 has a positive real eigenvalue and two complex-conjugate eigenvalues with negative real part. Otherwise, the Jacobian matrix at the equilibria P_2 and P_4 has one positive real eigenvalue and two negative real eigenvalues.

We prove Proposition 1 in Appendix A. We construct a region in the (u, v) plane for which the Jacobian matrix at the equilibria P_1 and P_3 has three real eigenvalues by performing numerical computations on the uniform grid points in the (u, v) plane. As one can see in Figure 1, the boundary of the region Γ_1 matches well with the boundary of the region that we obtain with numerical simulations. The same is true for the region Γ_2

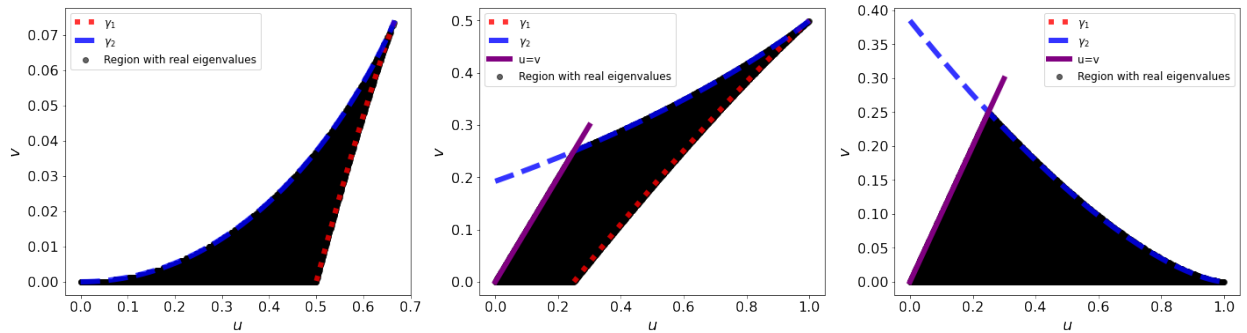


FIG. 1. The region Γ_1 in the (u, v) plane with (left) $m = 1$, (center) $m = 2$, and (right) $m = 0.5$. In this region, the Jacobian matrix at the equilibria P_1 and P_3 has real eigenvalues. We use γ_1 to denote the curve $u = v - \frac{(m+1 + \sqrt{4(m+1)^2 - 6m(v+2)})(\sqrt{4(m+1)^2 - 6m(v+2)} - 2(m+1))^2}{54m^2}$ and γ_2 to denote the curve $u = v - \frac{(m+1 - \sqrt{4(m+1)^2 - 6m(v+2)})(\sqrt{4(m+1)^2 - 6m(v+2)} + 2(m+1))^2}{54m^2}$.

III Dissipation and Contraction of the Dynamical System (6)–(8)

A dynamical system $\frac{d\vec{x}}{dt} = f(\vec{x})$ is dissipative if the volume of any fixed region in phase space contracts as a function of time. When the divergence $\nabla \cdot f < 0$ is constant, the volume contracts exponentially fast with a rate of $\nabla \cdot f$. In our case, calculating the divergence $\nabla \cdot f$ that is associated with equations (6)–(8) gives

$$\frac{\partial}{\partial \phi}(\gamma) + \frac{1}{m} \frac{\partial}{\partial \gamma}(-\gamma + \omega - k \sin \phi) + \frac{\partial}{\partial k}(\alpha \cos \phi - k) = -\frac{1}{m} - 1 < 0.$$

Therefore, our system is dissipative, with a volume contraction rate of $-\frac{1}{m} - 1$. For a dissipative system, all trajectories are eventually attracted to limiting sets of 0 measure and there are no quasiperiodic solutions.

All trajectories of (6)–(8) are eventually confined in a bounded region of phase space.

Theorem 1. *Suppose that $(\phi(t), \gamma(t), k(t))_{t \geq 0}$ is a trajectory of the dynamical system (6)–(8) and that $(\phi(0), \gamma(0), k(0)) = (\phi_0, \gamma_0, k_0)$. It is then the case that for all $\epsilon > 0$, there exists some time $T_\epsilon \geq 0$ such that $|k(t)| \leq \alpha + \epsilon$ and $|\gamma| \leq \omega + \alpha + \epsilon$ for all $t \geq T_\epsilon$.*

Proof. We start by multiplying both sides of (8) with the integrating factor e^t to obtain

$$\begin{aligned} \frac{d}{dt}(k(t)e^t) = \alpha \cos \phi(t)e^t &\implies k(t)e^t - k(0) = \int_0^t \alpha \cos \phi(\tilde{t})e^{\tilde{t}} d\tilde{t} \\ &\implies |k(t)e^t - k_0| \leq \int_0^t \alpha |\cos \phi(\tilde{t})|e^{\tilde{t}} d\tilde{t} \leq \int_0^t \alpha e^{\tilde{t}} d\tilde{t} = \alpha(e^t - 1). \end{aligned}$$

Consequently, $|k(t)| \leq \alpha + \frac{|k_0| - \alpha}{e^t} \leq \alpha + \epsilon$ for all $t \geq T_1 = \ln\left(\left|\frac{|k_0| - \alpha}{\epsilon}\right| + 1\right)$. Similarly, we multiply both sides of (7) with the integrating factor $e^{t/m}$ to obtain

$$\begin{aligned} \frac{d}{dt}(\gamma e^{t/m}) = \frac{\omega e^{t/m}}{m} - \frac{k(t)e^{t/m} \sin \phi(t)}{m} \\ \implies \gamma(t)e^{t/m} - \gamma_0 = \int_0^t \left[\frac{\omega e^{\tilde{t}/m}}{m} - \frac{k(\tilde{t})e^{\tilde{t}/m} \sin \phi(\tilde{t})}{m} \right] d\tilde{t}. \end{aligned}$$

Let $T_2 \in \mathbb{R}$ such that $|k(t)| \leq \alpha + \frac{\epsilon}{2}$ for all $t \geq T_2$. For all $t \geq T_2$, we then have

$$\begin{aligned}
\left| \gamma(t)e^{\frac{t}{m}} - \gamma_0 \right| &\leq \int_0^t \left| \frac{\omega e^{\tilde{t}/m}}{m} - \frac{k(\tilde{t})e^{\tilde{t}/m} \sin \phi(\tilde{t})}{m} \right| d\tilde{t} \\
&\leq \int_0^t \frac{\omega e^{\tilde{t}/m}}{m} d\tilde{t} + \int_0^t \frac{|k(\tilde{t})e^{\tilde{t}/m}|}{m} d\tilde{t} \\
&\leq \omega(e^{t/m} - 1) + \int_0^{T_2} \frac{|k(\tilde{t})e^{\tilde{t}/m}|}{m} d\tilde{t} + \int_{T_2}^t \frac{(\alpha + \frac{\epsilon}{2})e^{\tilde{t}/m}}{m} d\tilde{t} \\
&= \omega(e^{t/m} - 1) + \int_0^{T_2} \frac{|k(\tilde{t})e^{\tilde{t}/m}|}{m} d\tilde{t} + \left(\alpha + \frac{\epsilon}{2}\right)(e^{t/m} - e^{T_2/m}) \\
&= \left(\omega + \alpha + \frac{\epsilon}{2}\right)e^{t/m} - \omega - \left(\alpha + \frac{\epsilon}{2}\right)e^{T_2/m} + \int_0^{T_2} \frac{|k(\tilde{t})e^{\tilde{t}/m}|}{m} d\tilde{t}.
\end{aligned}$$

Consequently,

$$|\gamma(t)| \leq \left(\omega + \alpha + \frac{\epsilon}{2}\right) + \frac{\left| -\omega - \left(\alpha + \frac{\epsilon}{2}\right)e^{T_2/m} + \int_0^{T_2} \frac{|k(\tilde{t})e^{\tilde{t}/m}|}{m} d\tilde{t} + |\gamma_0| \right|}{e^{t/m}}.$$

The numerator of the second term is constant, so

$$\lim_{t \rightarrow \infty} \frac{\left| -\omega - \left(\alpha + \frac{\epsilon}{2}\right)e^{T_2/m} + \int_0^{T_2} \frac{|k(\tilde{t})e^{\tilde{t}/m}|}{m} d\tilde{t} + |\gamma_0| \right|}{e^{t/m}} = 0.$$

Therefore, there exists a constant $T_3 \in \mathbb{R}$ such that

$$\frac{\left| -\omega - \left(\alpha + \frac{\epsilon}{2}\right)e^{T_2/m} + \int_0^{T_2} \frac{|k(\tilde{t})e^{\tilde{t}/m}|}{m} d\tilde{t} + |\gamma_0| \right|}{e^{t/m}} \leq \frac{\epsilon}{2}$$

for all $t \geq T_3$. We conclude that $k(t) \leq \alpha + \epsilon$ and $\gamma(t) \leq \omega + \alpha + \epsilon$ for all $t \geq T_\epsilon = \max\{T_1, T_2, T_3\}$, as desired. \square

We now use an energy method to further examine the dynamical system (6)–(8). We define the energy

$$E(\phi, \gamma, k) := \frac{\alpha m \gamma^2}{2} - \alpha \omega \phi - \alpha k \cos \phi + \frac{k^2}{2}. \tag{15}$$

Consider the critical points of E . At these points,

$$\begin{aligned}
\frac{\partial E}{\partial \phi} = 0 &\implies -\alpha \omega + \alpha k \sin \phi = 0, \\
\frac{\partial E}{\partial \gamma} = 0 &\implies \alpha m \gamma = 0, \\
\frac{\partial E}{\partial k} = 0 &\implies -\alpha \cos \phi + k = 0.
\end{aligned}$$

We see that these three equations are the same equations for the equilibrium points of the dynamical system (6)–(8). Therefore, the equilibrium points are the critical points of E . In the interior of the domain $(\phi, \gamma, k) \in [-\pi, \pi) \times \mathbb{R} \times \mathbb{R}$, we calculate

$$\begin{aligned}
\frac{d}{dt}E(\phi, \gamma, k) &= \alpha m \gamma \frac{d\gamma}{dt} - \alpha \omega \frac{d\phi}{dt} - \alpha(-k \sin \phi \frac{d\phi}{dt} + \cos \phi \frac{dk}{dt}) + k \frac{dk}{dt} \\
&= \alpha m \gamma \frac{d\gamma}{dt} + (\alpha k \sin \phi - \alpha \omega) \frac{d\phi}{dt} + (k - \alpha \cos \phi) \frac{dk}{dt} \\
&= \alpha \gamma (-\gamma + \omega - k \sin \phi) + (\alpha k \sin \phi - \alpha \omega) \gamma + -(k - \alpha \cos \phi)^2 \\
&= -(\alpha \gamma^2 + (k - \alpha \cos \phi)^2) \leq 0.
\end{aligned}$$

We thus see that the energy of a trajectory of the dynamical system (6)–(8) never increases with time and that the time derivative of the energy is independent of m . However, a disadvantage of this energy function is that E is not 2π -periodic in ϕ (because of the $\alpha\omega\phi$ term). Therefore, the derivative of energy along the boundary of the domain in ϕ is not well-defined.

IV Demarcation of Different Qualitative Dynamics in the (α, ω) Plane

We simulate 50 trajectories of the dynamical system (6)–(8) with initial conditions that we choose uniformly at random in $[-\pi, \pi)^3$. For simplicity, we set the mass of each oscillator to $m = 1$. The domain of $\phi \in [-\pi, \pi)$ is exact, but the domain that we use for γ and k are arbitrary. By varying the learning enhancement factor α and the intrinsic-frequency difference ω , we obtain three regions Ω_1 , Ω_2 , and Ω_3 in the (α, ω) plane in which the trajectories exhibit qualitatively different dynamics.

In the region Ω_1 , the dynamical system (6)–(8) does not have any equilibrium points. Our simulations suggest that all trajectories converge to a periodic solution. See Figure 2 for an illustration. From equation (9), we infer that this region occurs for $0 < \alpha < 2\omega$. However, we have not proven rigorously that all trajectories converges to a single periodic solution or whether this periodic solution is a limit cycle. To gain insight into this periodic solution, we use an approximation. In [21], Menck et al. approximated solutions near a limit cycle of a second-order power grid model by assuming that oscillator phases rotate with a constant frequency of the limit cycle. Inspired by this idea, we suppose that there

exists $\zeta > 0$ (which we will determine later) for which $\phi(t) \approx \zeta t + \phi(0)$ and $\frac{d\phi}{dt} \approx \zeta$; we aim to parametrize $\gamma(t)$ and $k(t)$ by $\phi(t)$. Observe that equation (8) includes the term $\cos \phi$. Therefore, we posit an approximation of $k(t)$ of the form $k(t) \approx a \cos \phi(t) + b \sin \phi(t)$ for some constants a and b . Using the approximation $\frac{d\phi}{dt} \approx \zeta$ yields $\frac{dk}{dt} \approx (-a \sin \phi + b \cos \phi)\zeta$. Inserting the approximations of $k(t)$ and $\frac{dk}{dt}$ into equation (8) gives

$$(-a \sin \phi + b \cos \phi)\zeta + (a \cos \phi + b \sin \phi) \approx \alpha \cos \phi.$$

We now equate the coefficients of $\cos \phi$ and $\sin \phi$ to obtain $-a\zeta + b = 0$ and $b\zeta + a = \alpha$, and we then solve these two equations to obtain $a = \frac{\alpha}{\zeta^2 + 1}$ and $b = \frac{\alpha\zeta}{\zeta^2 + 1}$.

From equation (7) with $m = 1$, we have $\frac{d\gamma}{dt} + \gamma = \omega - k \sin \phi$. Similarly to our calculation above, we observe that equation (7) includes the term $k \sin \phi$. Recall from equation (6) that $\frac{d\phi}{dt} = \gamma$, so we posit an approximation of $\gamma(t)$ of the form $\gamma(t) \approx \zeta + c \cos 2\phi + d \sin 2\phi$ for some constants c and d . Inserting the approximations of $k(t)$ and $\gamma(t)$ into equation (7) with $m = 1$ yields

$$\begin{aligned} \zeta + (-2c\zeta + d) \sin 2\phi + (2d\zeta + c) \cos 2\phi &\approx \omega - \left(\frac{\alpha}{\zeta^2 + 1} \cos \phi + \frac{\alpha\zeta}{\zeta^2 + 1} \sin \phi \right) \sin \phi \\ &\approx \omega - \frac{\alpha}{2(\zeta^2 + 1)} \sin 2\phi - \frac{\alpha\zeta}{\zeta^2 + 1} \left(\frac{1 - \cos 2\phi}{2} \right) \\ &\approx \omega - \frac{\alpha\zeta}{2(\zeta^2 + 1)} - \frac{\alpha}{2(\zeta^2 + 1)} \sin 2\phi + \frac{\alpha\zeta}{2(\zeta^2 + 1)} \cos 2\phi. \end{aligned}$$

Equating the coefficients of $\cos 2\phi$ and $\sin 2\phi$ gives $\zeta = \omega - \frac{\alpha\zeta}{2(\zeta^2 + 1)}$, $-2c\zeta + d = -\frac{\alpha}{2(\zeta^2 + 1)}$, and $2d\zeta + c = \frac{\alpha\zeta}{2(\zeta^2 + 1)}$. Therefore, $c = \frac{3\zeta\alpha}{2(\zeta^2 + 1)(4\zeta^2 + 1)}$ and $d = \frac{(2\zeta^2 - 1)\alpha}{2(\zeta^2 + 1)(4\zeta^2 + 1)}$, where ζ is a real root of $2\zeta^3 - 2\omega\zeta^2 + (\alpha + 2)\zeta - 2\omega = 0$.

In summary, our approximation of our periodic solution satisfies

$$\begin{aligned} \phi(t) &\approx \zeta t + \phi(0), \\ \gamma(t) &\approx \zeta + \frac{3\zeta\alpha}{2(\zeta^2 + 1)(4\zeta^2 + 1)} \cos 2\phi(t) + \frac{(2\zeta^2 - 1)\alpha}{2(\zeta^2 + 1)(4\zeta^2 + 1)} \sin 2\phi(t), \\ k(t) &\approx \frac{\alpha}{\zeta^2 + 1} \cos \phi(t) + \frac{\alpha\zeta}{\zeta^2 + 1} \sin \phi(t), \end{aligned}$$

where ζ is a real root of $2x^3 - 2\omega x^2 + (\alpha + 2)x - 2\omega = 0$. We have checked numerically that this polynomial equation always has a single real root, so ζ is unique. As we can see in Figure 2, our approximate periodic solution is reasonably accurate. Furthermore, we have checked numerically that the phase difference ϕ increases approximately linear with respect to time. Therefore, we see that our assumptions approximately hold in practice.

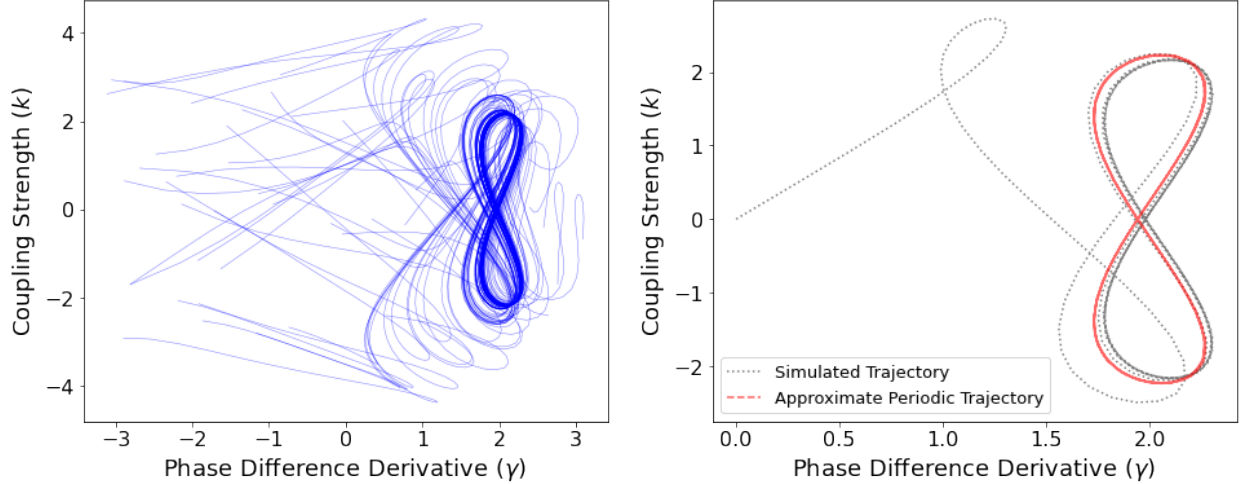


FIG. 2. Projection of simulated trajectories in the region Ω_1 for the dynamical system (6)–(8) with parameters $m = 1$, $\omega = 3$, and $\alpha = 5$ onto the (γ, k) plane. (Left) We simulate 50 trajectories with initial values that we choose uniformly at random in $[-\pi, \pi]^3$. (Right) We approximate the periodic trajectory that we observed in the region Ω_1 .

In the region Ω_2 , the dynamical system (6)–(8) has four equilibrium points in the domain $(\phi, \gamma, k) \in [-\pi, \pi) \times \mathbb{R} \times \mathbb{R}$. They are $P_1 = (\frac{1}{2} \arcsin(\frac{2\omega}{\alpha}), 0, \alpha \cos(\frac{1}{2} \arcsin(\frac{2\omega}{\alpha})))$, $P_2 = (\frac{\pi}{2} - \frac{1}{2} \arcsin(\frac{2\omega}{\alpha}), 0, \alpha \sin(\frac{1}{2} \arcsin(\frac{2\omega}{\alpha})))$, $P_3 = (-\pi + \frac{1}{2} \arcsin(\frac{2\omega}{\alpha}), 0, -\alpha \cos(\frac{1}{2} \arcsin(\frac{2\omega}{\alpha})))$, and $P_4 = (-\frac{\pi}{2} - \frac{1}{2} \arcsin(\frac{2\omega}{\alpha}), 0, -\alpha \sin(\frac{1}{2} \arcsin(\frac{2\omega}{\alpha})))$. In this region, there exists a heteroclinic orbit that connects the equilibrium points P_2 and P_4 . This situation is rather different from the periodic dynamics that we observed in the region Ω_1 . As one can see in our simulations in Figure 3, some trajectories converge to the equilibrium points but others converge to this heteroclinic orbit. By contrast, in region Ω_3 (see Figure 3), we observe that all simulated trajectories converge to the equilibrium points and that there is not a heteroclinic orbit. When we fix ω and gradually increase α , the behaviors of trajectories progress from the dynamics that we observe region Ω_1 to those that we observe in Ω_2 and finally to those in Ω_3 . Therefore, we conjecture that for each fixed ω , there exists a value α_ω of α such that the region Ω_2 corresponds to the region that is given by $2\omega \leq \alpha \leq \alpha_\omega$ and the region Ω_3 corresponds to the region for which $\alpha_\omega < \alpha$.

We seek to approximate the three regions Ω_1 , Ω_2 , and Ω_3 in the (α, ω) plane to gain insight into the quantity α_ω . We do this with numerical simulations and use the coarse method of checking whether or not there exists a heteroclinic orbit that connects P_2 and P_4 . We assume

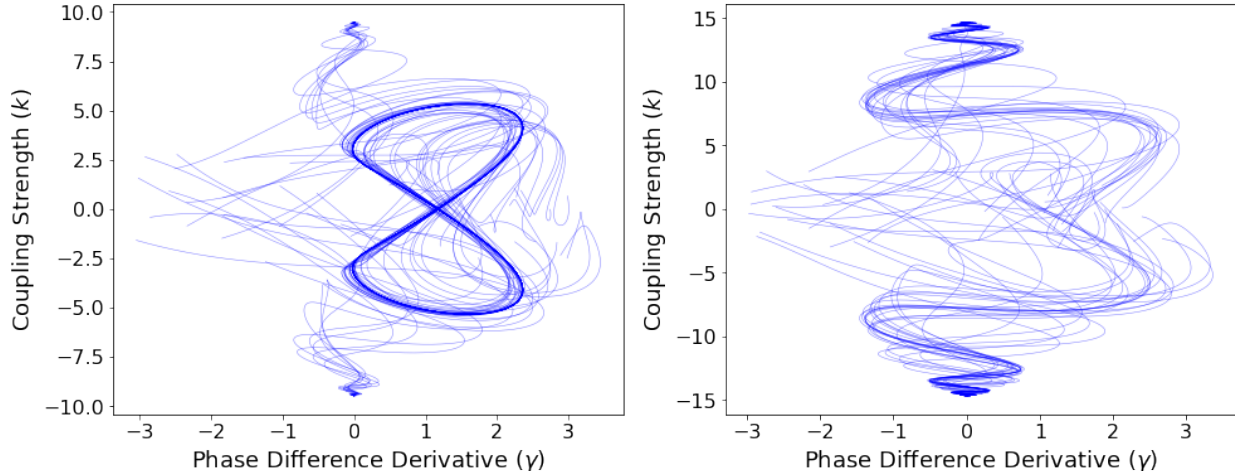


FIG. 3. (Left) Projection of simulated trajectories in the region Ω_2 for the dynamical system (6)–(8) with parameters $m = 1$, $\omega = 3$, and $\alpha = 10$ onto the (γ, k) plane. (Right) Projection of simulated trajectories in the region Ω_3 for the dynamical system (6)–(8) with parameters $m = 1$, $\omega = 3$, and $\alpha = 15$ onto the (γ, k) plane.

that $(\alpha, \omega) \in [0, 36] \times [0, 2\pi)$, and we then divide this rectangle into a grid with 150×150 points and consider the parameter values (α, ω) at each grid point. For each value of (α, ω) , because the phase ϕ has period 2π , we consider the Poincaré section $\mathcal{P} = \{(\phi, \gamma, k) | \phi = 0\}$. We pick 20 uniformly random initial values in the rectangle $R = \{0\} \times [-\pi, \pi] \times [-\pi, \pi]$ in \mathcal{P} . If the dynamical system (6)–(8) has a heteroclinic orbit, then it must pierce \mathcal{P} many times. Accordingly, we integrate for 1000 time steps for each initial condition, and we classify the ensuing region based on the mean number of times that a trajectory pierces \mathcal{P} . In practice, we find that if a trajectory converges to the equilibrium points, then it only pierces \mathcal{P} once or twice. Our approach only yields rough estimate of the regions Ω_1 , Ω_2 , and Ω_3 ; it does not precisely determine the boundaries between them.

V A Preliminary Investigation of the Dynamical System (1)–(2) with Many Oscillators

In Section IV, we observed that the qualitative dynamics of trajectories of the 3D system (6)–(8) depend on the oscillators’ intrinsic-frequency difference ω and the learning enhancement factor α . We now use these insights to motivate our preliminary investigate of the

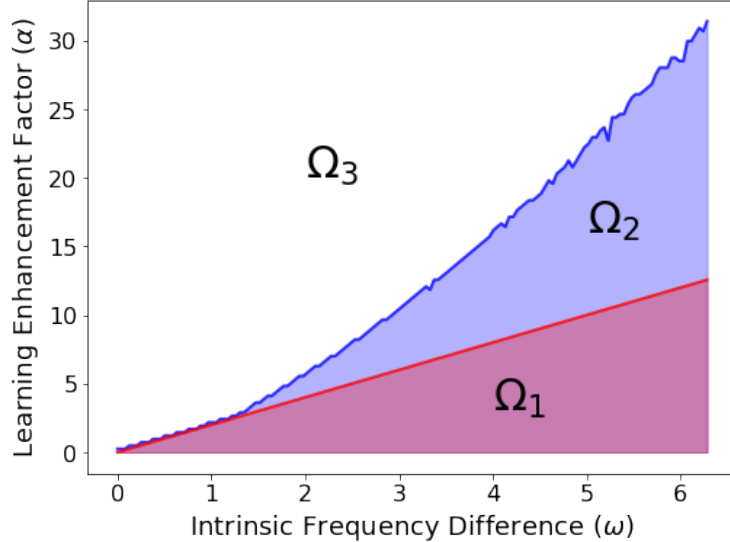


FIG. 4. Approximate regions in the (α, ω) plane for which the dynamical system (6)–(8) has different dynamical properties.

general equations (1)–(2) for the Kuramoto model with inertia and Hebbian learning.

We consider a specific setup for the intrinsic oscillator frequencies ω_i (with $i \in \{1, \dots, N\}$) by sampling them randomly from a Gaussian distribution with 0 mean and several variances $\mathcal{N}(0, \sigma^2)$. We expect that the variance σ^2 in the high-dimensional system (1)–(2) will play a role that is analogous to the intrinsic-frequency difference ω in the 3D system (6)–(8). As was noted in [16], the existence of Hebbian-learning interactions can result in multiple phase-locked clusters of oscillators. To take the possibility of two phase-locked clusters of oscillators into account, we calculate the order parameter

$$r_2(t) = \left| \frac{1}{N} \sum_{j=1}^N e^{2\phi_j(t)i} \right|. \quad (16)$$

We perform numerical simulations to investigate how $r_2(t)$ changes with time. For simplicity, we consider a system of $N = 50$ oscillators with homogeneous mass $m = 1$. This yields a dynamical system of $\frac{50(51)}{2} = 1275$ coupled differential equations. We set the initial phases of each oscillator uniformly in $[0, 2\pi)$, so $\phi_i(0) = \frac{2\pi i}{N}$. We choose the initial phase derivatives to be $\phi'_i(0) = 0$, and we choose the initial coupling strengths to be $K_{ij} = 1$. We consider two schemes to investigate the effects of α and σ^2 on the order parameter $r_2(t)$ by fixing one of the two parameters and varying the another. We show our results in Figure 5.

The oscillators are incoherent when $\sigma^2 \gg \alpha$, and they in two phase-locked clusters when

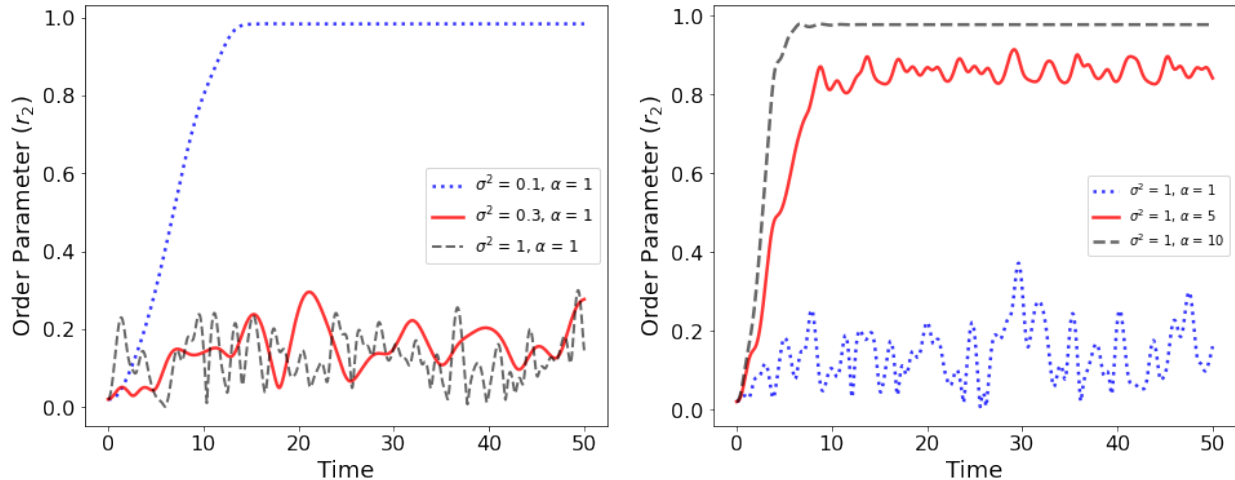


FIG. 5. The order parameter $r_2(t)$ of the system (1)–(2) with $N = 50$ oscillators that each have a mass of $m = 1$. (Left) We fix the learning enhancement factor $\alpha = 1$ and consider variances of $\sigma^2 = 0.1$, $\sigma^2 = 0.3$, and $\sigma^2 = 1$. (Right) We fix a variance of 1 and consider $\alpha = 1$, $\alpha = 5$, and $\alpha = 10$.

$\alpha \gg \sigma^2$. When we fix σ^2 and vary α , we see three distinct qualitative dynamics of r_2 . When α is small relative to σ^2 , the system is in an incoherent state in which r_2 oscillates near 0. As we increase the value of α , a larger fraction of the oscillators becomes phase-locked and r_2 oscillates around a positive value. Eventually, when α is sufficiently large, r_2 no longer oscillates and instead attains a constant value that is near 1. These three types of qualitative dynamics in the high-dimensional system (1)–(2) are similar to the three regions Ω_1 , Ω_2 , and Ω_3 that we observed in the 3D system (6)–(8). In the high-dimensional system, for fixed values of σ^2 and ω , as we increase the value of α , the incoherent set of oscillators experiences progressively more phase-locking until eventually most oscillators are in one of two phase-locked clusters. In the low-dimensional system, for fixed values of σ^2 and ω , as we increase the value of α , progressively fewer trajectories converge to a periodic solution and instead converge to the equilibrium points P_1 or P_3 .

VI Conclusions

We studied an adaptive Kuramoto model with inertia in which the coupling strengths between phase oscillators depend on a Hebbian learning rule. We focused our analysis on

the situation with $N = 2$ coupled oscillators, for which the dynamical system is three-dimensional system. We examined the equilibrium points of this system and studied their linear stabilities. We showed that all of this system's trajectories are eventually confined in a bounded region and then investigated the attractor of this system. Using numerical simulations, we found three different types of qualitative dynamics, where the regions in which they occur depend on a learning enhancement factor α and the intrinsic-frequency difference ω between the two oscillators. We then used numerical computations to approximate the boundaries between these regions.

Our insights from the 3D system suggested a choice for the oscillators' intrinsic frequencies in high-dimensional situations. We selected these frequencies from a Gaussian distribution with 0 mean and different variances. We found that the variance of the oscillators' intrinsic frequencies in the high-dimensional system plays a role that is similar to the intrinsic-frequency difference ω in the low-dimensional system. As we vary the parameter α , we observed that the high-dimensional system of coupled oscillators transitions from an incoherent state into partial phase-locked states and finally to a state with two almost fully phase-locked clusters.

In neuroscience, long-term potentiation (LTP) synapses and long-term depression (LDP) synapses, respectively, refer to types of synapses in which presynaptic neurons repeatedly promote or inhibit postsynaptic neurons [22]. In a model of a neuronal system as a set of coupled oscillators, LTP describes a situation in which all oscillators are in-phase and LDP describes a situation in which all oscillators are in anti-phase [16]. Based on (1) our observation that the trajectories in our 3D system converge either to a periodic orbit or to one of two equilibrium points and (2) our definition of the order parameter $r_2(t)$, which captures the synchrony of two phase-locked clusters of oscillators, our Kuramoto model with inertia and Hebbian learning suggests that the behaviors of the oscillators are analogous to those of LTP and LDP synapses in neuronal networks.

A natural extension of our work is to undertake a thorough analysis of how changes in inertia affect the transition to phase-locked groups of oscillators as one varies the parameters. In the 3D system (6)–(8), it seems worthwhile to obtain an analytical approximation for how the boundary between regions Ω_2 and Ω_3 changes with respect to changes in inertia. We hope that a further understanding on the demarcation between regions Ω_2 and Ω_3 can provide further insight into the qualitative dynamics in different regions of parameter space for the

high-dimensional system (1)–(2).

A Appendix A

In this appendix, we prove Proposition 1.

Proposition 1. *Consider the dynamical system (6)–(8) with $\alpha > 2\omega$. Let $u := \alpha + \sqrt{\alpha^2 - 4\omega^2}$ and $v := \alpha - \sqrt{\alpha^2 - 4\omega^2}$. The following statements hold:*

1. Let Γ_1 be the region in the (u, v) plane with $0 \leq v \leq u \leq \frac{2(m^2-m+1)}{3m}$ that is bounded by the curves

$$v = u - \frac{(m+1 + \sqrt{4(m+1)^2 - 6m(u+2)})(\sqrt{4(m+1)^2 - 6m(u+2)} - 2(m+1))^2}{54m^2},$$

$$v = u - \frac{(m+1 - \sqrt{4(m+1)^2 - 6m(u+2)})(\sqrt{4(m+1)^2 - 6m(u+2)} + 2(m+1))^2}{54m^2}.$$

If $(u, v) \notin \Gamma_1$, then the Jacobian matrix at the equilibria P_1 and P_3 has a negative real eigenvalue and two complex-conjugate eigenvalues with negative real part. Otherwise, the Jacobian matrix at the equilibria P_1 and P_3 has three negative real eigenvalues.

2. Let Γ_2 be the region in the (u, v) plane with $0 \leq v \leq u$ and $v \leq \frac{2(m^2-m+1)}{3m}$ that is bounded by the curves

$$u = v - \frac{(m+1 + \sqrt{4(m+1)^2 - 6m(v+2)})(\sqrt{4(m+1)^2 - 6m(v+2)} - 2(m+1))^2}{54m^2},$$

$$u = v - \frac{(m+1 - \sqrt{4(m+1)^2 - 6m(v+2)})(\sqrt{4(m+1)^2 - 6m(v+2)} + 2(m+1))^2}{54m^2}.$$

If $(u, v) \notin \Gamma_2$, the Jacobian matrix at the equilibria P_2 and P_4 has a positive real eigenvalue and two complex-conjugate eigenvalues with negative real part. Otherwise, the Jacobian matrix at the equilibria P_2 and P_4 has one positive real eigenvalue and two negative real eigenvalues.

Proof. We first consider the region Γ_1 , which is the region in the (α, ω) plane for which the equilibria P_1 and P_3 have three negative real eigenvalues. From equation (12), we need to consider the values of α and ω for which the polynomial

$$f(x) = 2x(x+1)(mx+1) + (\alpha + \sqrt{\alpha^2 - 4\omega^2})(x+1) - (\alpha - \sqrt{\alpha^2 - 4\omega^2})$$

$$= 2mx^3 + 2(m+1)x^2 + (u+2)x + u - v$$

has three real roots. When $\alpha > 2\omega \geq 0$, we have that $u \geq v \geq 0$ are real. Therefore, because $f(x)$ is a degree-3 polynomial with real coefficients, it must have either three real roots or

one real root and two complex-conjugate roots. The boundary of the region Γ_1 occurs when $f(x)$ has a double root \tilde{x} . Therefore, we also consider

$$f'(x) = 6mx^2 + 4(m+1)x + u + 2.$$

The root \tilde{x} must be a root of both $f(x) = 0$ and $f'(x) = 0$, so it must be a root of

$$Q(x) = 3f(x) - xf'(x) = 2(m+1)x^2 + 2(u+2)x + 3(u-v) = 0.$$

We obtain \tilde{x} by solving

$$0 = (m+1)f'(\tilde{x}) - 3mQ(\tilde{x}) = (4(m+1)^2 - 6(u+2)m)\tilde{x} - (9m(u-v) - (u+2)(m+1))$$

to yield

$$\tilde{x} = \frac{9m(u-v) - (u+2)(m+1)}{4(m+1)^2 - 6(u+2)m}.$$

The value \tilde{x} must also be a root of $f'(x) = 0$, so

$$\tilde{x} = \frac{9m(u-v) - \left(\frac{4(m+1)^2 - s}{6m}\right)(m+1)}{s} = \frac{-(m+1) \pm 2\sqrt{s}}{12m}, \quad (\text{A1})$$

where $s := 4(m+1)^2 - 6(u+2)m$. Rearranging equation (A1) yields

$$u - v = \frac{\pm s\sqrt{s} - 3s(m+1) + 4(m+1)^3}{54m^2} = \frac{(\pm\sqrt{s} + m+1)(\sqrt{s} \mp 2(m+1))^2}{54m^2}. \quad (\text{A2})$$

The choice of signs in (A2) gives the two boundary curves in the proposition. For \tilde{x} to be a real number, we require that $s \geq 0$, so $u \geq \frac{2(m^2 - m + 1)}{3m}$. We obtain equation (13) by swapping the variables u and v in equation (12). We then obtain the boundary curves of the region Γ_2 using the same calculation with u and v swapped.

Observe that $f(0) = 2\sqrt{\alpha^2 - 4\omega^2}$ and that $f(-1) = -(\alpha - \sqrt{\alpha^2 - 4\omega^2})$. Consequently, by the Intermediate Value Theorem, there exists a real root in the interval $[-1, 0)$. Furthermore, by Vieta's Theorem, we also know that the sum of these roots is -2 . Therefore, the eigenvalues of the Jacobian matrix at the equilibria P_1 and P_3 all have negative real parts. Similarly, let $g(x) := -2x(x+1)^2 - (\alpha - \sqrt{\alpha^2 - 4\omega^2})(x+1) + (\alpha + \sqrt{\alpha^2 - 4\omega^2})$ be the left-hand side of equation (13). Observe that $g(0) = 2\sqrt{\alpha^2 - 4\omega^2} > 0$ and that $g\left(\frac{2\sqrt{\alpha^2 - 4\omega^2}}{\alpha - \sqrt{\alpha^2 - 4\omega^2}}\right) = -\frac{4\sqrt{\alpha^2 - 4\omega^2}(\alpha + \sqrt{\alpha^2 - 4\omega^2})}{(\alpha - \sqrt{\alpha^2 - 4\omega^2})^2} < 0$. Therefore, by the Intermediate Value Theorem, there exists a positive real root in the interval $(0, \frac{2\sqrt{\alpha^2 - 4\omega^2}}{\alpha - \sqrt{\alpha^2 - 4\omega^2}})$. Furthermore, by Vieta's Theorem, we also know that the sum of these roots of g is -2 . Therefore, the Jacobian matrix at the equilibria P_2 and P_4 has a positive real eigenvalue and two eigenvalues with negative real parts. □

Acknowledgements

We thank Predrag Cvitanović for helpful discussions.

- [1] A. Pikovsky and M. Rosenblum, Synchronization, *Scholarpedia* **2**, 1459 (2007).
- [2] P. Mateos-Aparicio and A. Rodríguez-Moreno, The impact of studying brain plasticity, *Frontiers in Cellular Neuroscience* **13**, 402 (2019).
- [3] G. B. Ermentrout, An adaptive model for synchrony in the firefly *Pteroptyx malaccae*, *Journal of Mathematical Biology* **29**, 571–585 (1991).
- [4] S. H. Strogatz, From Kuramoto to Crawford: Exploring the onset of synchronization in populations of coupled oscillators, *Physica D* **143**, 1 (2000).
- [5] R. E. Mirollo and S. H. Strogatz, Synchronization of pulse-coupled biological oscillators, *SIAM Journal on Applied Mathematics* **50**, 1645–1662 (1990).
- [6] S. H. Strogatz, D. M. Abrams, A. McRobie, B. Eckhardt, and E. Ott, Crowd synchrony on the Millennium Bridge, *Nature* **438**, 43–44 (2005).
- [7] I. Belykh, M. Bocian, A. R. Champneys, K. Daley, R. Jeter, J. H. G. Macdonald, and A. McRobie, Emergence of the London Millennium Bridge instability without synchronisation, *Nature Communications* **12**, 7223 (2021).
- [8] D. C. Michaels, E. P. Matyas, and J. Jalife, Mechanisms of sinoatrial pacemaker synchronization: A new hypothesis, *Circulation Research* **61**, 704–714 (1987).
- [9] K. Ota, I. Aihara, and T. Aoyagi, Interaction mechanisms quantified from dynamical features of frog choruses, *Royal Society Open Science* **7**, 191693 (2020).
- [10] Y. Kuramoto, *Chemical Oscillations, Waves, and Turbulence* (Springer-Verlag, Heidelberg, Germany, 1984).
- [11] F. Rodrigues, T. K. D. Peron, P. Ji, and J. Kurths, The Kuramoto model in complex networks, *Physics Reports* **610**, 1 (2016).
- [12] B. R. Trees, V. Saranathan, and D. Stroud, Synchronization in disordered Josephson junction arrays: Small-world connections and the Kuramoto model, *Physical Review E* **71**, 016215 (2005).

- [13] M. Rohden, A. Sorge, M. Timme, and D. Witthaut, Self-organized synchronization in decentralized power grids, *Physical Review Letters* **109**, 064101 (2012).
- [14] H.-A. Tanaka, A. J. Lichtenberg, and S. Oishi, Self-synchronization of coupled oscillators with hysteretic responses, *Physica D* **100**, 279–300 (1997).
- [15] D. O. Hebb, *The Organization of Behavior* (John Wiley and Sons, Inc., Hoboken, NJ, USA, 1964).
- [16] R. K. Niyogi and L. Q. English, Learning-rate-dependent clustering and self-development in a network of coupled phase oscillators, *Physical Review E* **80**, 066213 (2009).
- [17] L. Timms and L. Q. English, Synchronization in phase-coupled Kuramoto oscillator networks with axonal delay and synaptic plasticity, *Physical Review E* **89**, 032906 (2014).
- [18] P. Seliger, S. C. Young, and L. S. Tsimring, Plasticity and learning in a network of coupled phase oscillators, *Physical Review E* **65**, 041906 (2002).
- [19] Q. Ren and J. Zhao, Adaptive coupling and enhanced synchronization in coupled phase oscillators, *Physical Review E* **76**, 016207 (2007).
- [20] S.-Y. Ha, S. E. Noh, and J. Park, Synchronization of Kuramoto oscillators with adaptive couplings, *SIAM Journal on Applied Dynamical Systems* **15**, 162–194 (2016).
- [21] P. J. Menck, J. Heitzig, J. Kurths, and H. J. Schellnhuber, How dead ends undermine power grid stability, *Nature Communications* **5**, 3969 (2014).
- [22] T. V. P. Bliss and S. F. Cooke, Long-term potentiation and long-term depression: A clinical perspective, *Clinics* **66**, 3 (2011).